Above-room-temperature coupling between ferroelastic domains and magnetism in an organic-inorganic hybrid: $CsCu(HCOO)_2Cl$

Junyan Zhou,[1,2] Shifeng Jin,[1,2,*] Ruijin Sun,[3] Congcong Chai,[1,4] Munan Hao,[1,2] Xin Zhong,[1] and Xiaolong Chen[1,2,5,†]

[1]*Beijing National Laboratory for Condensed Matter Physics, Institute of Physics, Chinese Academy of Sciences, Beijing 100190, China*

[2]*School of Physical Sciences, University of Chinese Academy of Sciences, Beijing 101408, China*

[3]*School of Science, China University of Geosciences, Beijing 100083, China*

[4]*College of Materials Science and Opto-Electronic Technology, University of Chinese Academy of Sciences, Beijing 101408, China*

[5]*Songshan Lake Materials Laboratory, Dongguan 523808, China*

(Received 14 February 2021; accepted 24 June 2021; published 14 July 2021)

Coupling between ferroelastic domains and magnetism (CFM) is usually observed in ferromagnetic phases where an easily magnetized direction can change with the movement of ferroelastic domains. Organic-inorganic hybrids (OIHs) are expected to enhance the coupling due to their low elastic modules. However, it is challenging to find CFM above room temperature in OIHs since the magnetic orderings are generally at low temperatures. The occurrence of CFM without magnetic ordering remains a question. Here, we report an interesting OIH: $CsCu(HCOO)_2Cl$, where canted antiferromagnetic and ferroelastic ordering occur at 32 and 331 K, respectively. Induced by Cu dimers, $CsCu(HCOO)_2Cl$ shows large magnetic anisotropy at room temperature, the strength of which is twice that below 32 K. It is an example of an OIH showing that ferroelastic domains can couple with magnetism above room temperature. Moreover, our findings present a way to realize room-temperature CFM in OIHs and enhance our understanding of CFM.

DOI: 10.1103/PhysRevMaterials.5.074405

I. INTRODUCTION

In ferroelastic materials, there are ferroelastic domains with different orientations that can be changed under mechanical stresses. If these domains exhibit magnetic anisotropy, it will enable the magnetic susceptibility to be manipulated by mechanical stress. This coupling between ferromagnetism and ferroelastic domains has been found in a few alloys and oxides such as Ni-Mn-Ga, Ni-Fe-Ga, Ni-Co-Mn-In, and $LaCo_xSr_{1-x}O_3$ [1–4]. In the past decade, organic-inorganic hybrid compounds (OIHs) have been extensively studied due to their various physical properties combined with the advantages of environmental friendliness, easy preparation, and mechanical flexibility [5–9]. Compared with traditional inorganic counterparts, the OIH ferroelastics require smaller forces for the twinning deformation [7]. If their ferromagnetism can be coupled by ferroelastic domains, enhanced coupling between ferroelastic domains and magnetism (CFM) is expected. However, this coupling has been rarely reported in OIHs. Recently, a layered OIH perovskite, $(C_6H_5C_2H_4NH_3)_2FeCl_4$, was found to exhibit both canted antiferromagnetism and ferroelasticity. The large magnetic anisotropy and the orientation of ferroelastic domains exactly match along the [100] and [010] directions; therefore, coupling between the two ferroic states was observed [10]. Nevertheless, such coupling is only reported below the magnetic transition temperature of 98 K. Owing to the generally low temperatures of magnetic ordering [11–13], it is extremely difficult to find OIHs with both magnetic and ferroelastic ordering around room temperature. A recent study indicates that magnetic ordering can exist at up to 515 K in OIHs [14], but without ferroelastic ordering.

In ferromagnets or canted antiferromagnets, the existence of easy magnetization axes usually results in magnetic anisotropy. In OIHs, polynuclear transition metals and organic ligands form atomic clusters that connect each other in three directions. Inside the clusters, magnetic moments of metal ions strongly interact with each other, but long-range intracluster magnetic ordering can only form at low temperatures because the adjacent clusters are too far apart [15–17]. It has been shown, however, that magnetic anisotropy can still exist above ordering temperatures. The reason is that polynuclear transition metals can lead to nondegenerate orbital angular momenta and large zero-field splitting (ZFS) that are direction dependent and can persist above room temperature [18,19]. Intuitively, the magnetic anisotropy can be equally coupled by ferroelastic domains. This means that OIHs are candidates possessing CFM at room temperature.

A ferroelastic usually undergoes a structural phase transition accompanying changes in the crystal system. Such a phase transition should involve displacement, rotation, or ordering of atomic clusters in OIHs. This demands that the atomic clusters are small enough in size. This is the main reason why ferroelasticity is rarely found in OIHs containing polynuclear transition metals. From this point of view, dimeric tetracarboxylate paddle-wheel motifs of the general formula $M_2(COO)_4$ [13] are good candidates to be included in OIHs. In these motifs, the two metal ions are connected by four carboxylate ions. Meanwhile, large magnetic anisotropy has been observed at room temperature in compounds containing $M_2(COO)_4$ [16]. As the simplest carboxylate ion, connecting

*shifengjin@iphy.ac.cn
†chenx29@iphy.ac.cn

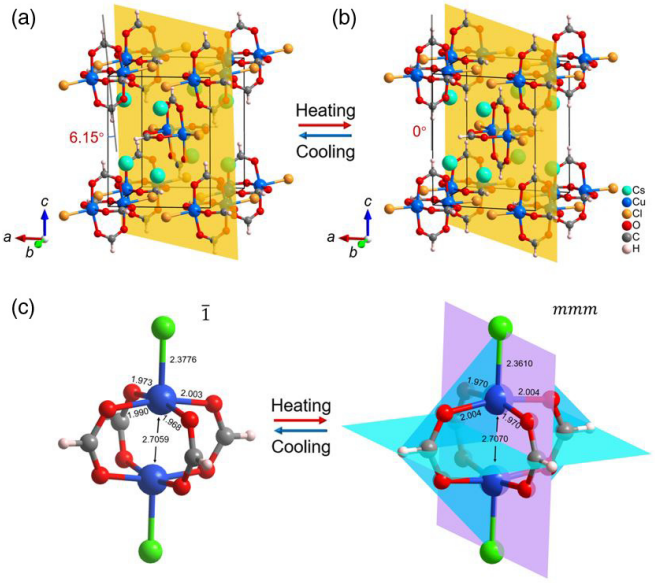

FIG. 1. Structures of $CsCu(HCOO)_2Cl$ at (a) 300 K and (b) 335 K. The Cs-Cl and Cs-O bonds are hidden for clarity. To clearly show the rotation of the Cu dimer during the phase transformation, the (110) crystal planes are presented; the rotation angle is 6.15°. (c) Structure and selected bond lengths (unit: Å) of Cu dimers in the ferroelastic phase and the paraelastic phase. During the phase transition, the symmetry of the Cu dimers changes from $\bar{1}$ to *mmm*. The planes represent the mirror planes of the Cu dimer in the paraelastic phase.

the two metal ions by formate ions will greatly reduce the size of the atomic cluster, making it possible to realize room-temperature CFM.

In this work, we successfully synthesized a multiferroic compound $CsCu(HCOO)_2Cl$ that undergoes a magnetic phase transition at 32 K and another one from ferro- to paraelastic at 331 K. Magnetic anisotropy emerges because of the anisotropic Landé g factor and ZFS in triplet Cu dimers: $[Cu_2(HCOO)_4Cl_2]^{2-}$. We show that the ferroelastic domains are not only coupled with the long-range magnetic ordering state at low temperatures, but also with magnetic anisotropy above room temperature. Our findings demonstrate that CFM can be realized via non-long-range magnetic ordering and highlight the importance of magnetic anisotropy in OIHs in this regard.

II. STRUCTURE AND PHASE TRANSITION

Differential scanning calorimetry (DSC) measurements for $CsCu(HCOO)_2Cl$ show there are an endothermic peak at 331 K during the heating process and an exothermic one at 328 K during the cooling process, respectively (Fig. S5(a) in the Supplemental Material [20]; also see [21–28]), indicating a first-order phase transition occurs, where ΔH is about 0.351 kJ/mol. Powder x-ray diffractions (PXRDs) measured at 300 and 335 K reveal that the phase transition transits structural transformation (Fig. S6(b) [20]). The crystal structures of both phases were solved and refined based on the single-crystal x-ray diffraction data collected at 300 and 335 K. As shown in Fig. 1, a pair of Cu^{2+} ions, four $HCOO^-$ ions, and two Cl^- ions form a paddle-wheel-like structure unit with the two Cu^{2+} ions connected by formate ions. Such metal dimers connected by carboxyls have been reported in many OIHs [29–32]. Each Cs^+ ion is bonded to four dimers through Cs-Cl and Cs-O bonds. At 300 K, $CsCu(HCOO)_2Cl$ crystallizes in a monoclinic cell with a space group of $P2_1/n$; the spacings of Cu-O, Cu-Cl, and Cu-Cu are $1.968 \sim 2.003$, 2.3776, and 2.7059 Å, respectively; and the bond angles of Cl-Cu-O are 94.16°–99.21°. Each cell contains two Cu dimers and four Cs^+ ions, i.e., four chemical formulas. At 335 K, the symmetry changes to $P4_2/mnm$. The spacings of Cu-O, Cu-Cl, and Cu-Cu change to 1.970–2.004 Å, 2.3610 Å, and 2.7070 Å. The bond angles of Cl-Cu-O range from 96.84° to 96.86°, suggesting that the paddle-wheel-like copper dimers become more symmetrical. Meanwhile, the position of the Cs^+ ion moves to a high-symmetry position (0.5, 0, 0.25), which is on the 4_2 axis. Such a symmetry change between $P4_2/mnm$ and $P2_1/n$ is characterized by a ferroelastic phase transition of $4/mmmF2/m(s)$ type as described by Aizu [33]. Here, "s" represents that the twofold axis of the point symmetry $2/m$ in the low-temperature phase corresponds to one of the twofold axes perpendicular to the fourfold axis of the point symmetry $4/mmm$ in the high-temperature phase. The ferroelastic phase transition temperature determined by DSC is 331 K, indicating that $CsCu(HCOO)_2Cl$ is a room-temperature ferroelastic.

III. FERROELASTICITY

Point group $4/mmm$ can be regarded as the direct product of point group $2/m$ and 4, implying that ferroelastic domains with four orientations satisfying the symmetry of 4 will appear in a single crystal (Fig. S1). To visualize the ferroelastic domains, variable temperature polarization microscopy was performed on a single crystal (Fig. 2). The (011) plane of the single crystal was used for observation. When the polarizers were removed, the crystal surface showed a plane with uniform color and brightness. Under polarizers, dark parallelograms appeared. Then the sample was heated to 340 K, and the parallelograms disappeared, as a typical feature of a phase transition from ferroelastic to paraelastic. Returning to room temperature, the domains reappeared, indicating that the crystal returned to the ferroelastic phase. For the ferroelastic phase transitions belonging to Aizu species $4/mmmF2/m(s)$, the strain tensor of the four orientation states has the form [21]

$$X_S(S_1) = \begin{bmatrix} \frac{e_{11}-e_{22}}{2} & 0 & e_{13} \\ 0 & \frac{e_{22}-e_{11}}{2} & 0 \\ e_{13} & 0 & 0 \end{bmatrix},$$

$$X_S(S_2) = \begin{bmatrix} \frac{e_{22}-e_{11}}{2} & 0 & 0 \\ 0 & \frac{e_{11}-e_{22}}{2} & e_{13} \\ 0 & e_{13} & 0 \end{bmatrix},$$

$$X_S(S_3) = \begin{bmatrix} \frac{e_{11}-e_{22}}{2} & 0 & -e_{13} \\ 0 & \frac{e_{22}-e_{11}}{2} & 0 \\ -e_{13} & 0 & 0 \end{bmatrix},$$

$$X_S(S_4) = \begin{bmatrix} \frac{e_{22}-e_{11}}{2} & 0 & 0 \\ 0 & \frac{e_{11}-e_{22}}{2} & -e_{13} \\ 0 & -e_{13} & 0 \end{bmatrix}, \quad (1)$$

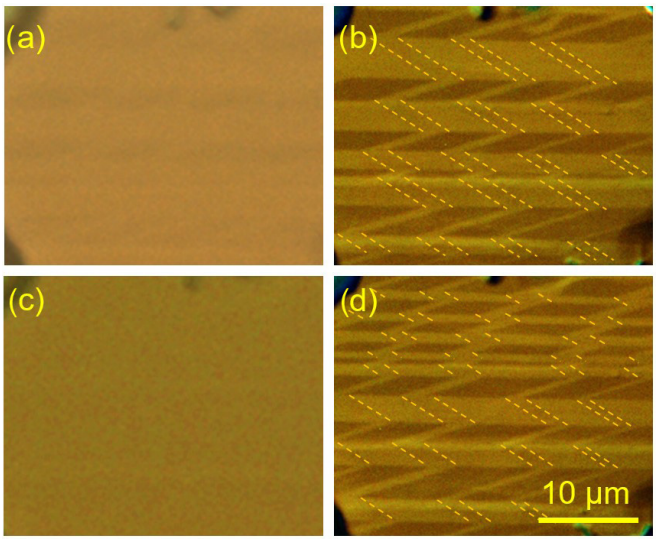

FIG. 2. Ferroelastic domains in the (011) plane of a thermally treated single crystal. (a) Photograph under natural polarized light. (b) Photograph at room temperature under polarized light. (c) Photograph after heating to 340 K under polarized light. (d) Photograph after cooling from 340 K to room temperature under polarized light. Some imperceptible domain walls are marked with dashed lines. All photographs were collected in the same area with the same scale bar.

where e_{11}, e_{22}, e_{13} can be calculated by cell parameters of the ferroelastic and paraelastic phases,

$$e_{11} = \frac{a_F}{a_P} - 1, \quad e_{11} = \frac{b_F}{b_P} - 1, \quad e_{13} = \tan\frac{1}{2}(\beta - 90^\circ). \tag{2}$$

The magnitude of spontaneous strain is defined by

$$X_S = \left[\sum_{i,j} X_{Sij}^2(S_k)\right]^{\frac{1}{2}} = 0.0392. \tag{3}$$

Such a value is similar to those of other OIH ferroelastics, such as [DMICE]Cd(SCN)$_3$ (0.0379) [34], [(CH$_3$)$_3$PCH$_2$OH]CdBr$_3$ (0.0457) [35], and [(CH$_3$)$_4$P]Cd(SCN)$_3$ (0.0622) [36].

IV. MAGNETISM

Dimeric transition metal tetracarboxylates, $M_2(COO)_4$, often form a paddle-wheel-like atomic cluster and are the origin for interesting magnetic properties in OIHs [13]. CsCu(HCOO)$_2$Cl is found to exhibit rich magnetic properties. Temperature-dependent magnetizations of a powder sample are shown in Fig. 3(a). It is obvious that there are two magnetic phase transitions at about 8 and 32 K. The splitting of magnetization curves under zero-field cooling (ZFC) and field cooling (FC) indicates that the transition at 32 K (T_N) is due to magnetic ordering. Magnetic hysteresis loops are observed at 5 and 20 K in the isothermal magnetization measurements, and coercive fields are estimated to be 59 and 363 Oe, respectively. The spontaneous magnetizations of Cu^{2+} ions are estimated to be 4.47×10^{-4} and $1.07 \times 10^{-4}\mu_B$, which are much smaller than the theoretical saturation moment $1.73\mu_B$. Such low spontaneous magnetizations suggest that the magnetic moments of CsCu(HCOO)$_2$Cl below 32 K are in a slightly canted antiferromagnetic state. The transition at 8 K can be attributed to the change of the average canting angle, from 0.015° (5 K) to 0.004° (20 K). At 40 K, the *M-H* curve becomes a straight line, suggesting that the long-range magnetic ordering disappears. However, the magnetism is not paramagnetic as usual. During the heating process, the magnetization decreases with the temperature until 117 K, and then increases. This abnormal magnetization-temperature (*M-T*) behavior also appears in other OIHs containing $Cu_2(COO)_4$ groups such as $Cu_2(1,3\text{-bdc})_2(py)_2$ [37], $Cu_3(1,3,5\text{-btc})_2(H_2O)_3$ [38], and $Cu_2(bptc)(H_2O)_3(DMF)_3$ [39]. Such behavior can be explained by a competitive mechanism. On the one hand, the ground state of each independent Cu dimer is a spin singlet ($S = 0$) due to the strong antiferromagnetic interaction. With increasing temperature, some singlet states are excited to triplet states ($S = 1$), the contribution of this part makes the susceptibility increase. Such an excitation was probed by electron paramagnetic resonance (Fig. S2 in the Supplemental Material [20]); similar results have also been found in $[Cu_2(tert\text{-}Bupy)_4(N_3)_2](ClO_4)_2$ [40], $[(PhCO_2)_4(DMSO)_2]Cu_2$ [41], and $[Cu(C_6H_5COO)_2(C_6H_5(OH)CONH_2)]_2$ [22]. On the other hand, there is negligible magnetic interaction between different Cu dimers above T_N. Therefore, the spin orientation of excited triplet states should be random, like the so-called superparamagnetism. This makes the susceptibility decrease with the increase of temperature. It is easily known that the energy gap E_g between the singlet state and the triplet state of a Cu dimer should be larger than $4k_BT_\theta$, where k_B is the Boltzmann constant and T_θ is the Weiss temperature of Cu dimers; the derivation is shown in the Supplemental Material [20]. No saturation in susceptibility at room temperature suggests that the energy gap E_g in CsCu(HCOO)$_2$Cl is large (see the Supplemental Material) [20].

V. COUPLING BETWEEN MAGNETISM AND FERROELASTIC DOMAINS

To characterize the correlation between ferroelastic domains and magnetism, the temperature-dependent moment of a single-domain crystal under $H = 1$ T along [010] was measured [Fig. 3(c)]. Firstly, the temperature was reduced to 5 K; the magnetic susceptibility curve was similar to that of the powder with rising temperature. However, when the temperature rose to 329 K, which was close to the structural phase transition temperature, the magnetic susceptibility had a steplike increase. After that, the magnetic susceptibility continued to rise slowly. In the cooling process, at first, the magnetic susceptibility decreased slowly and coincided with the heating process until the temperature dropped to 329 K. Unexpectedly, there was no steplike decrease in magnetic susceptibility. Moreover, the magnetic susceptibility no longer coincided with the heating process, ruling out the possibility of magnetic phase transition being induced by structural phase transition. This unexpected phenomenon can be explained

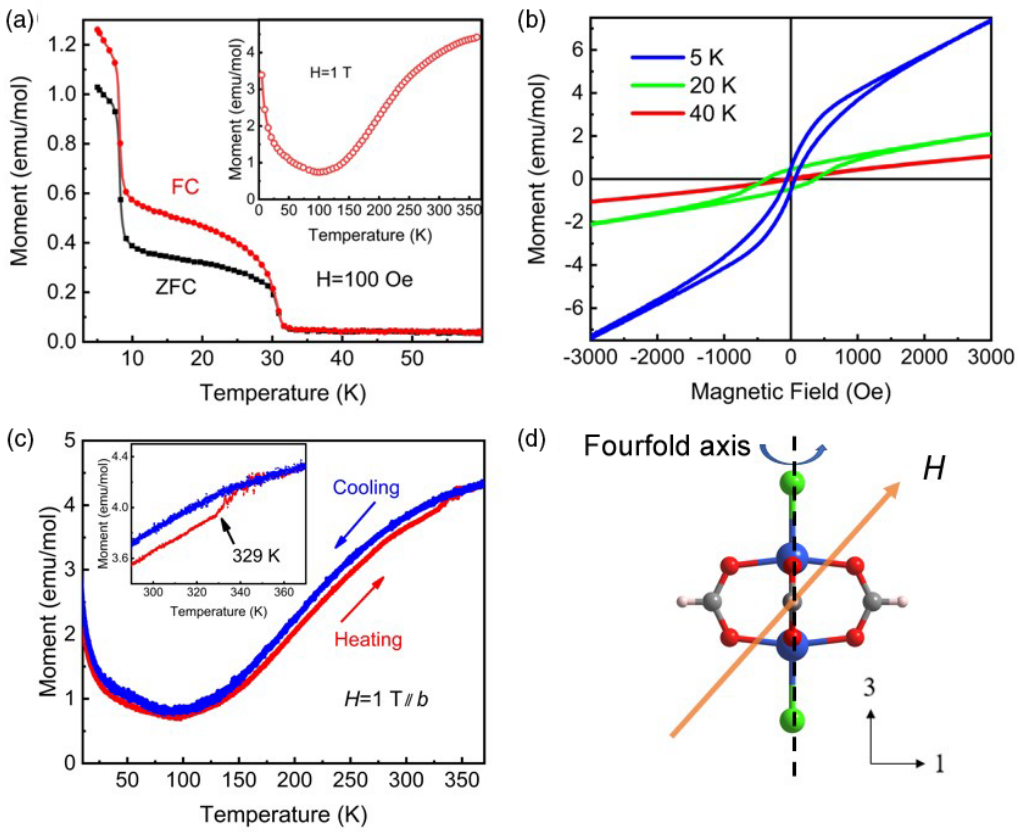

FIG. 3. Magnetism of $CsCu(HCOO)_2Cl$. (a) Moment as a function of temperature under a magnetic field of 100 Oe (powder sample). Inset: Temperature-dependent moment from 5 to 363 K under a magnetic field of 1 T. (b) Isothermal magnetization curves at 5, 20, and 40 K (powder sample). The three temperatures correspond to the three magnetic phases determined by variable temperature magnetization measurement. (c) Temperature-dependent moment curves of a single crystal under a magnetic field of 1 T during a heating and cooling cycle; the direction of given magnetic field is along the b axis. Inset: the details around the ferroelastic-paraelastic phase transition. (d) Schematic diagram of a Cu dimer under a magnetic field along the b axis, where the dashed line represents the assumed fourfold axis of the Cu dimer, and "1" and "3" represent the two axes of the coordinate system based on a Cu dimer.

by the magnetic anisotropy of a ferroelastic domain and the irreversibility of domain distributions during a heating and cooling cycle.

The magnetic anisotropy of the crystal can be ascribed to the orientation and arrangement of Cu dimers. From the crystal structure we solved, the anisotropic magnetic susceptibility of the crystal (300 K) can be expressed by that of the Cu dimer:

$$
\begin{aligned}
{}^{F}\chi_{aa} &= 0.9797\chi_{11} + 1.0203\chi_{33} \\
{}^{F}\chi_{bb} &= 1.0220\chi_{11} + 0.9780\chi_{33}.
\end{aligned} \tag{4}
$$

Here, the Cu dimer is assumed to have a fourfold axis [Fig. 3(d)] and χ_{11}, χ_{33} are the magnetic susceptibilities perpendicular and parallel to the fourfold axis of the Cu dimer, respectively. The details of the derivation are shown in the Supplemental Material [20]. In a single-domain crystal, the magnetic susceptibility of the [010] direction is smaller than that of the [100] direction, and is also smaller than that of the [100] direction of the tetragonal phase; in other words, ${}^{F}\chi_{bb} < {}^{F}\chi_{aa}$ and ${}^{F}\chi_{bb} < {}^{P}\chi_{aa}$. If the temperature reaches 329 K in the heating process, the magnetization vector $\boldsymbol{M}$ will jump from ${}^{F}\chi_{bb}\boldsymbol{H}$ to ${}^{P}\chi_{aa}\boldsymbol{H}$, while in the cooling process, the crystal changes from the paraelastic state to the ferroelastic state around 329 K, and will not return to the initial single-domain state, but into a multidomain state. The distribution of ferroelastic domains in the [100] and [010] orientations were random. Such a domain distribution gives a total magnetization $({}^{F}\chi_{aa} + {}^{F}\chi_{bb})\boldsymbol{H}/2$. The magnetization difference between heating and cooling at 300 K is 0.171 emu/mol; the value ${}^{F}\chi_{aa} - {}^{F}\chi_{bb}$ at 300 K can be estimated to be 4.17×10^{-6} (in the International System of Units). It can be inferred that $({}^{F}\chi_{aa} + {}^{F}\chi_{bb})/2 \approx {}^{P}\chi_{aa}$ around 329 K, because there is no magnetic susceptibility jump during the cooling process. The coexistence of magnetic anisotropy and ferroelastic ordering implies that the magnetic susceptibility can be controlled by mechanical stress.

The change of magnetic anisotropy during the ferroelastic-paraelastic phase transition can be detected by angle-dependent torque measurements [42,43]. The torque is defined as $\boldsymbol{\tau}(\varphi) = \mu_0 V \boldsymbol{M} \times \boldsymbol{H}$, where φ is the angle between the magnetic field and the a axis of the crystal, μ_0 is the permeability of vacuum, and V is the sample volume. The relationship of the rotation direction and the c axis obeys the right-handed rule. In this geometry, the component along the axis of rotation of $\boldsymbol{\tau}(\varphi)$ is a periodic function

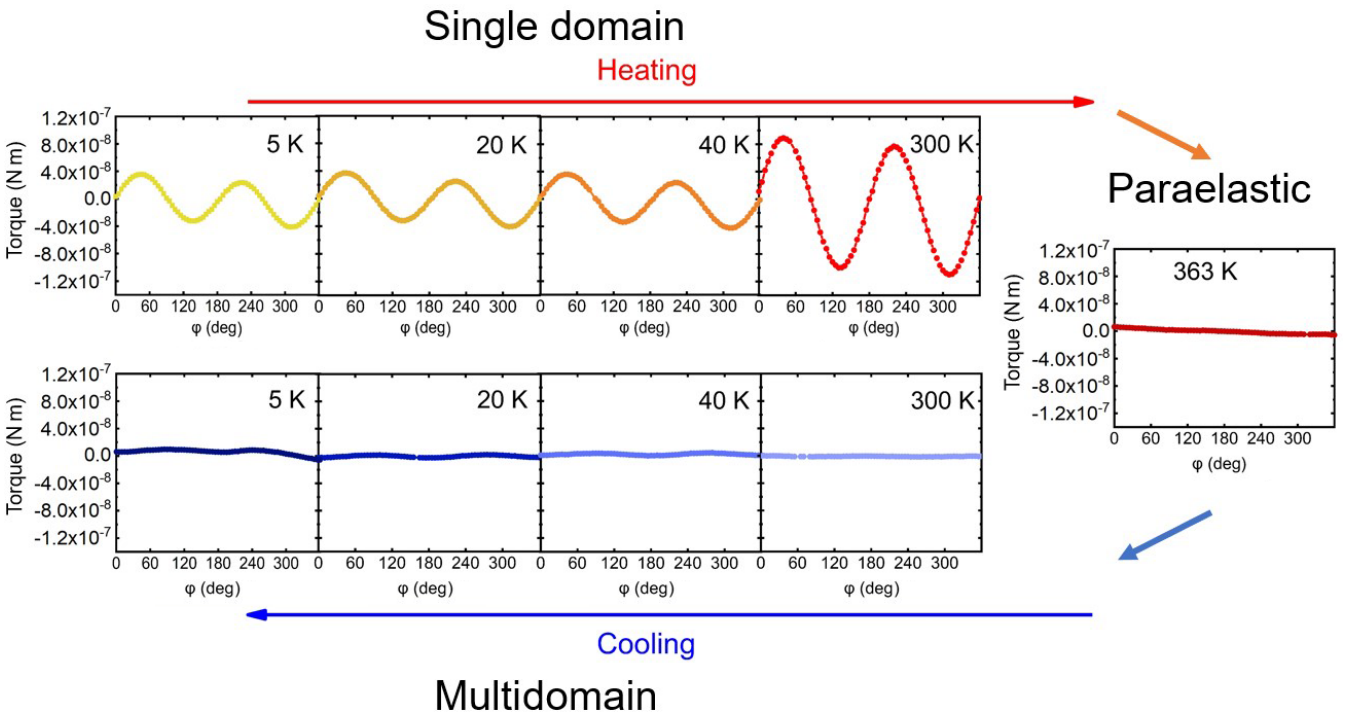

FIG. 4. Angle-dependent magnetic torque under 5 T at different temperatures during a heating and cooling cycle. The rotation axis is along the *c* axis and the magnetic field is parallel to the *ab* plane. Obvious magnetic anisotropy is observed at 5, 20, 40, and 300 K during the heating process, corresponding to the ferroelastic single-domain phase. The absence of magnetic anisotropy at 363 K can be ascribed to the symmetry of the tetragonal system, in other words, the paraelastic phase. The absence of magnetic anisotropy at 300, 40, 20, and 5 K during the cooling process, corresponding to the ferroelastic multidomain phase.

of 2φ [44–46]. That is,

$$\tau_c = \tfrac{1}{2}\mu_0 V H^2[(\chi_{aa} - \chi_{bb})\sin 2\varphi - 2\chi_{ab}\cos 2\varphi]. \quad (5)$$

In both the monoclinic and tetragonal crystal systems, χ_{ab} is zero due to the symmetry; then τ_c becomes

$$\tau_c = \tfrac{1}{2}\mu_0 V H^2(\chi_{aa} - \chi_{bb})\sin 2\varphi. \quad (6)$$

From Eq. (6), it can be seen that if the magnetic anisotropy between the [100] and [010] directions exists, τ_c will be a sine function of 2φ; otherwise, τ_c is zero. A single-domain crystal was selected for torque-angle measurement at a series of temperatures 5, 20, 40, 300, and 363 K during both the heating and cooling processes (Fig. 4). Clearly, sine curves were observed at 5, 20, 40, and 300 K during the heating process, which suggests the existence of magnetic anisotropy in the single-domain state. Besides, these curves indicate that the value of $\chi_{aa} - \chi_{bb}$ is positive, which is consistent with our previous analysis. The amplitude of the 300 K curve is about 9.0×10^{-8} N m, from which the value $\chi_{aa} - \chi_{bb}$ is calculated to be 4.62×10^{-6}, agreeing well with the magnetization measurements. It should be noted that the value of $\chi_{aa} - \chi_{bb}$ at room temperature is higher than that at low temperature (in the canted antiferromagnetic phase). This phenomenon is different from other compounds with paramagnetic anisotropy [47–49]. Considering that the dimer number excited to the triplet state will increase with temperature, the larger magnetic anisotropy at room temperature can be attributed to the fact that the magnetic anisotropy mainly comes from the triplet states of Cu dimers. At 363 K and 300, 40, 20, and 5 K during the cooling process, where the crystal was in the paraelastic state and the ferroelastic multidomain state, respectively, τ_c almost did not change with the angle, which strongly supports the coupling between magnetism and ferroelastic domains.

VI. CONCLUSIONS

In summary, an OIH compound $CsCu(HCOO)_2Cl$ exhibiting complex magnetism and room-temperature ferroelasticity is reported. Due to the magnetic anisotropy between the [100] and [010] directions without magnetic ordering, it is possible to manipulate magnetism by controlling ferroelastic domains with mechanical stress at room temperature. This is an example that CFM can occur at room temperature in OIHs. Moreover, By combining ferroelasticity with magnetic anisotropy of polynuclear transition metals, more and more OIHs with higher-temperature and stronger CFM could be found soon. For the increasing demand for flexible and low-cost devices, it can be anticipated that such coupling in OIHs will be applied in the near future.

ACKNOWLEDGMENTS

This work is financially supported by the National Key Research and Development Program of China (Grants No. 2018YFE0202600 and No. 2016YFA0300301); the National Natural Science Foundation of China under Grants No. 51532010, No. 91422303, and No. 51772323; and the Key Research Program of Frontier Sciences, CAS, Grant No. QYZDJ-SSW-SLH013.

[1] K. Ullakko, J. K. Huang, C. Kantner, R. C. O'Handley, and V. V. Kokorin, Appl. Phys. Lett. **69**, 1966 (1996).

[2] K. Oikawa, T. Ota, T. Ohmori, Y. Tanaka, H. Morito, A. Fujita, R. Kainuma, K. Fukamichi, and K. Ishida, Appl. Phys. Lett. **81**, 5201 (2002).

[3] R. Kainuma, Y. Imano, W. Ito, Y. Sutou, H. Morito, S. Okamoto, O. Kitakami, K. Oikawa, A. Fujita, T. Kanomata, and K. Ishida, Nature **439**, 957 (2006).

[4] T. Kyômen, A. Sano, Y. Murachi, M. Hanaya, K. Suzuki, and M. Ito, Phys. Rev. B **82**, 064402 (2010).

[5] W. Yuan, Y. Zeng, Y. Y. Tan, J. H. Zhou, W. J. Xu, W. X. Zhang, and X. M. Chen, Chem. Commun. **55**, 8983 (2019).

[6] V. B. Jakobsen, E. Trzop, L. C. Gavin, E. Dobbelaar, S. Chikara, X. Ding, K. Esien, H. Muller-Bunz, S. Felton, V. S. Zapf, E. Collet, M. A. Carpenter, and G. G. Morgan, Angew. Chem., Int. Ed. Engl. **59**, 13305 (2020).

[7] T. Seki, C. Feng, K. Kashiyama, S. Sakamoto, Y. Takasaki, T. Sasaki, S. Takamizawa, and H. Ito, Angew. Chem., Int. Ed. Engl. **59**, 8839 (2020).

[8] W. J. Xu, Y. Zeng, W. Yuan, W. X. Zhang, and X. M. Chen, Chem. Commun. **56**, 10054 (2020).

[9] H. Y. Zhang, C. L. Hu, Z. B. Hu, J. G. Mao, Y. Song, and R. G. Xiong, J. Am. Chem. Soc. **142**, 3240 (2020).

[10] Y. Nakayama, S. Nishihara, K. Inoue, T. Suzuki, and M. Kurmoo, Angew. Chem., Int. Ed. Engl. **56**, 9367 (2017).

[11] J. S. Miller, Chem. Soc. Rev. **40**, 3266 (2011).

[12] D. F. Weng, Z. M. Wang, and S. Gao, Chem. Soc. Rev. **40**, 3157 (2011).

[13] A. E. Thorarinsdottir and T. D. Harris, Chem. Rev. **120**, 8716 (2020).

[14] P. Perlepe, I. Oyarzabal, A. Mailman, M. Yquel, M. Platunov, I. Dovgaliuk, M. Rouzieres, P. Negrier, D. Mondieig, E. A. Suturina, M. A. Dourges, S. Bonhommeau, R. A. Musgrave, K. S. Pedersen, D. Chernyshov, F. Wilhelm, A. Rogalev, C. Mathoniere, and R. Clerac, Science **370**, 587 (2020).

[15] T. Kajiwara, M. Nakano, Y. Kaneko, S. Takaishi, T. Ito, M. Yamashita, A. Igashira-Kamiyama, H. Nojiri, Y. Ono, and N. Kojima, J. Am. Chem. Soc. **127**, 10150 (2005).

[16] W. Z. Chen, F. A. Cotton, N. S. Dalal, C. A. Murillo, C. M. Ramsey, T. Ren, and X. Wang, J. Am. Chem. Soc. **127**, 12691 (2005).

[17] R. Bagai and G. Christou, Chem. Soc. Rev. **38**, 1011 (2009).

[18] T. O. Strandberg, C. M. Canali, and A. H. MacDonald, Nat. Mater. **6**, 648 (2007).

[19] M. Nakano and H. Oshio, Chem. Soc. Rev. **40**, 3239 (2011).

[20] See Supplemental Material at http://link.aps.org/supplemental/10.1103/PhysRevMaterials.5.074405 for details of sample preparation, crystal structure determination, thermal measurements, polarizing microscopy, magnetic measurements, calculation of ferroelastic spontaneous strain, evidence for the excited triplet, phenomenological explanation of the M-T curves above T_N, relationship between the magnetic anisotropy of Cu dimers, and the magnetic anisotropy of crystal. Also see Refs. [21–28].

[21] K. Aizu, J. Phys. Soc. Jpn. **28**, 706 (1970).

[22] H. Phetmung and A. Nucharoen, Polyhedron **173**, 114121 (2019).

[23] G. M. Sheldrick, Acta Crystallogr., Sect. A **64**, 112 (2008).

[24] J. L. de Miranda, J. Felcman, M. H. Herbst, and N. V. Vugman, Inorg. Chem. Commun. **11**, 655 (2008).

[25] M. Šimėnas, M. Kobalz, M. Mendt, P. Eckold, H. Krautscheid, J. Banys, and A. Pöppl, J. Phys. Chem. C **119**, 4898 (2015).

[26] P. M. Selvakumar, E. Suresh, S. Waghmode, and P. S. Subramanian, J. Coord. Chem. **64**, 3495 (2011).

[27] B. Kozlevčar, I. Leban, M. Petrič, S. Petriček, O. Roubeau, J. Reedijk, and P. Šegedin, Inorg. Chim. Acta **357**, 4220 (2004).

[28] J. Moncol, M. Mudra, P. Lönnecke, M. Hewitt, M. Valko, H. Morris, J. Svorec, M. Melnik, M. Mazur, and M. Koman, Inorg. Chim. Acta **360**, 3213 (2007).

[29] G. Arribas, M. C. Barral, R. Gonzalez-Prieto, R. Jimenez-Aparicio, J. L. Priego, M. R. Torres, and F. A. Urbanos, Inorg. Chem. **44**, 5770 (2005).

[30] M. Dan and C. N. Rao, Angew. Chem., Int. Ed. Engl. **45**, 281 (2005).

[31] B. H. Brodsky and J. Du Bois, Chem. Commun. **2006**, 4715 (2006).

[32] S. Xiang, W. Zhou, J. M. Gallegos, Y. Liu, and B. Chen, J. Am. Chem. Soc. **131**, 12415 (2009).

[33] K. Aizu, Phys. Rev. B **2**, 754 (1970).

[34] L. He, L. Zhou, P. P. Shi, Q. Ye, and D. W. Fu, Chem. Mater. **31**, 10236 (2019).

[35] X. Zheng, L. Zhou, P. P. Shi, F. J. Geng, D. W. Fu, and Q. Ye, Chem. Commun. **53**, 7756 (2017).

[36] Y. J. Cao, L. Zhou, P. P. Shi, Q. Ye, and D. W. Fu, Chem. Commun. **55**, 8418 (2019).

[37] B. Moulton, J. Lu, R. Hajndl, S. Hariharan, and M. J. Zaworotko, Angew. Chem., Int. Ed. Engl. **41**, 2821 (2002).

[38] X. X. Zhang, S. S. Y. Chui, and I. D. Williams, J. Appl. Phys. **87**, 6007 (2000).

[39] L. Shen, S. W. Yang, S. Xiang, T. Liu, B. Zhao, M. F. Ng, J. Goettlicher, J. Yi, S. Li, L. Wang, J. Ding, B. Chen, S. H. Wei, and Y. P. Feng, J. Am. Chem. Soc. **134**, 17286 (2012).

[40] M. L. Boillot, Y. Journaux, A. Bencini, D. Gatteschi, and O. Kahn, Inorg. Chem. **24**, 263 (2002).

[41] Y. Reyes-Ortega, J. L. Alcantara-Flores, M. C. Hernandez-Galindo, D. Ramirez-Rosales, S. Bernes, J. C. Ramirez-Garcia, R. Zamorano-Ulloa, and R. Escudero, J. Am. Chem. Soc. **127**, 16312 (2005).

[42] C. Rossel, P. Bauer, D. Zech, J. Hofer, M. Willemin, and H. Keller, J. Appl. Phys. **79**, 8166 (1996).

[43] E. Ohmichi and T. Osada, Rev. Sci. Instrum. **73**, 3022 (2002).

[44] R. Okazaki, T. Shibauchi, H. J. Shi, Y. Haga, T. D. Matsuda, E. Yamamoto, Y. Onuki, H. Ikeda, and Y. Matsuda, Science **331**, 439 (2011).

[45] Y. Sato, S. Kasahara, H. Murayama, Y. Kasahara, E. G. Moon, T. Nishizaki, T. Loew, J. Porras, B. Keimer, T. Shibauchi, and Y. Matsuda, Nat. Phys. **13**, 1074 (2017).

[46] H. Murayama, Y. Sato, R. Kurihara, S. Kasahara, Y. Mizukami, Y. Kasahara, H. Uchiyama, A. Yamamoto, E. G. Moon, J. Cai, J. Freyermuth, M. Greven, T. Shibauchi, and Y. Matsuda, Nat. Commun. **10**, 3282 (2019).

[47] L. Holmes, R. Sherwood, L. G. Van Uitert, and S. Hüfner, Phys. Rev. **178**, 576 (1969).

[48] P. D. W. Boyd, D. A. Buckingham, R. F. McMeeking, and S. Mitra, Inorg. Chem. **18**, 3585 (2002).

[49] Z. He and Y. Ueda, Phys. Rev. B **77**, 220406 (2008).